Pergamon

0301-9322(95)00024-0

Int. J. Multiphase Flow Vol. 21, No. 5, pp. 893–906, 1995

0301-9322/95 $9.50 + 0.00

EXPERIMENTAL STUDIES ON A CO-CURRENT GAS–LIQUID DOWNFLOW BUBBLE COLUMN

G. KUNDU, D. MUKHERJEE† and A. K. MITRA
Department of Chemical Engineering, Indian Institute of Technology, Kharagpur 721 302, India

(Received 3 April 1994; in revised form 15 March 1995)

Abstract—Two-phase co-current vertical downflow systems offer some distinct advantages, like uniform and finer bubbles, greater residence time, negligible coalescence of the bubbles etc. In the present work the hydrodynamics of a vertical downflow bubble column fitted with an ejector have been evaluated. Experimental studies have been carried out to evaluate the total pressure gradient and gas holdup. Similarity analysis was used for analysing the data in order to overcome the complex flow behaviour in the system. Correlations have been developed to predict pressure drop and holdup of gas as a function of different physical and dynamic variables.

Key Words: two-phase, downflow, bubble column, pressure drop, gas holdup

1. INTRODUCTION

A myriad of studies have been reported on the hydrodynamics of two-phase co-current flow. The majority of these studies deal with either horizontal two-phase flow or vertical two-phase upflow. Studies reported with a two-phase vertical downflow system are very meagre. These studies can be categorized either under a plunging jet or sparger type system. In a plunging jet system, a jet of liquid, while plunging into a pool of the same liquid, carries along with it some ambient gas which disperses into bubbles due to the momentum transfer of the jet. The liquid and bubbles move down in the liquid pool to some distance and the gas bubbles then move up. Research papers published on the plunging jet system are those of Burgess *et al.* (1972), Burgess & Molloy (1973), Van de Sande & Smith (1976), Van de Donk *et al.* (1979), Schügerl (1985) etc. These studies are highly encouraging and are said to be energetically attractive but the major drawbacks in this system are: co-current downflow of a gas and liquid is limited to a short distance depending upon the jet momentum and the time of contact of the gas and liquid is also short.

In a sparger type system, the gas sparger is fixed at the top of the column and liquid with a high velocity is forced through the column. The liquid shears the gas from the sparger in the form of bubbles and then moves down as a two-phase flow. In this system it is very difficult to obtain a stable flow and, according to Kulkarni & Shah (1984) and Bando *et al.* (1988), the range of meaningful operation is quite narrow. Reported studies with sparger type downflow systems are those of Herbrechtsmeier *et al.* (1981), Rao *et al.* (1983), Kulkarni & Shah (1984), Ohkawa *et al.* (1985) etc. Studies have also been reported in a downflow bubble column with a simultaneous gas–liquid injection nozzle by Ben Brahim *et al.* (1984), Bando *et al.* (1988) and Velan & Ramanujam (1991).

The two-phase vertical downflow system has some distinct advantages, viz. bubbles are finer and more uniform in size, coalescence of the bubbles is negligible, homogenization of the two phases in the column is possible, gas–liquid contact is more and a very small amount of gas can be dispersed. In recent years the two-phase downflow system has attracted the attention of researchers, hence a system which simultaneously gives the effect of a plunging jet as well as that of a sparger type system has been developed. In this system, a liquid jet ejector has been fitted to the vertical column and the present study deals with the analysis of the pressure drop and holdup of a co-current, gas–liquid two-phase downflow bubble column.

†To whom correspondence should be addressed.

2. EXPERIMENTAL APPARATUS

A schematic diagram of the experimental set-up is shown in figure 1. It consists of an ejector assembly, E, an extended pipe line contractor, C, a gas–liquid separator, SE, and other accessories like a centrifugal pump, PU, a pressure gauge, P, manomenters, M_1–M_9, control valves, V_1–V_9, quick closing solenoid valves, SV_1–SV_3, a rotameter, R, a thermometer, Th, and a storage tank, T. For visual observation of the flow the ejector assembly and extended contactor were made of perspex having a 51.6 mm i.d. and 2030 mm length. The major dimensions of the apparatus are given in table 1. In the present set-up the optimum dimensions of the ejector were used as reported by Mukherjee *et al.* (1988). The forcing nozzle, N, is of the straight hole type and is precision-bored to obtain a smooth passage and to avoid any undue shock or losses. The dimensions of the nozzles are given in table 2. An extended pipe line contactor, C, was provided below the ejector assembly as shown in figure 1 for gas–liquid two-phase downflow. The lower end of the contactor projected 300 mm into the separator, SE. This arrangement enabled uniform movement of the two-phase downflow and also easy separation of the bubbles from the main stream. The air–liquid separator is a rectangular mild steel vessel of 320 × 320 mm size and 855 mm height and was sufficiently large

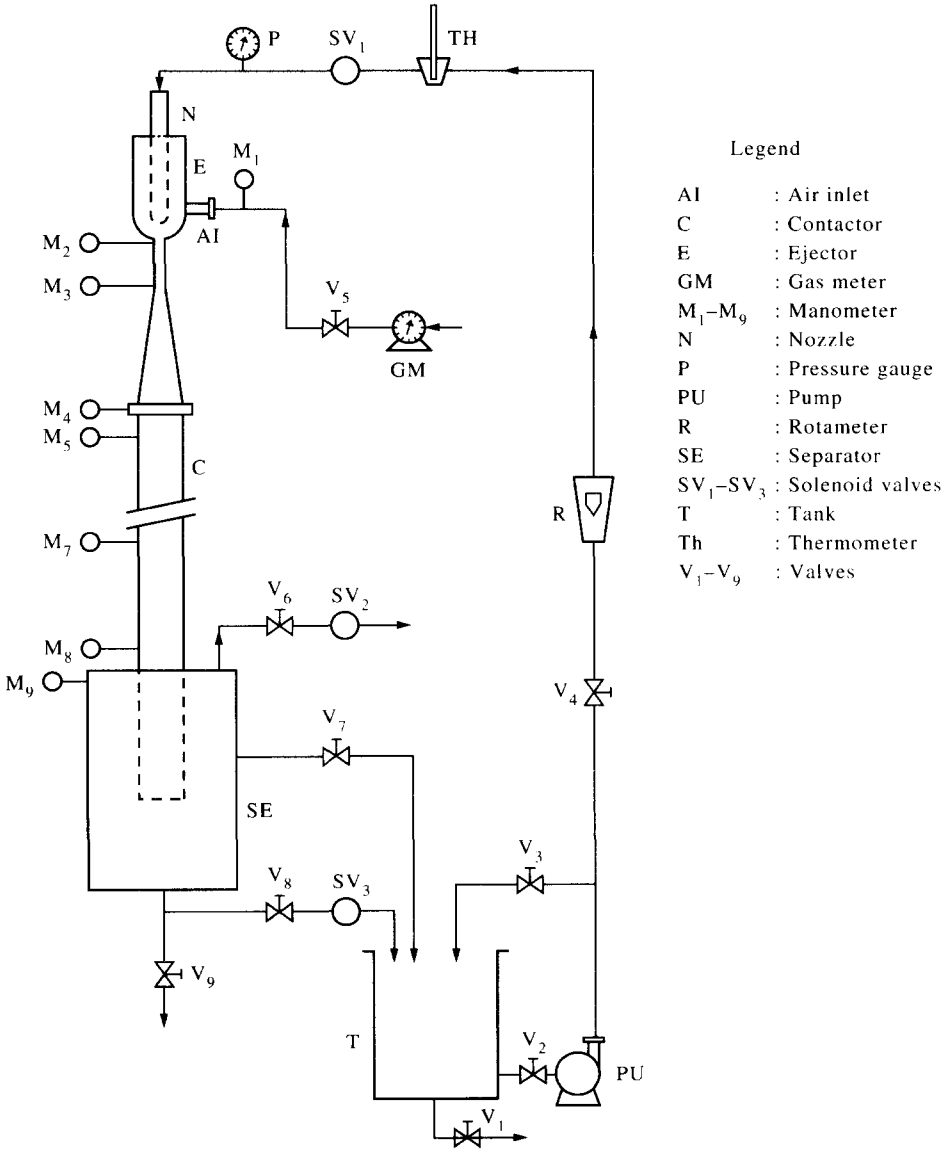

Figure 1. Schematic diagram of the experimental set-up.

Table 1. Dimensions of the ejector–contactor assembly

Sl. No.	Description	Dimensions in mm
1	Diameter of the throat, d_t	19.0
2	Length of the throat, L_t	184.0
3	Angle of divergence of the diffuser	7°
7	Length of the divergent diffuser, L_d	204.0
5	Diameter of the contactor, d_c	51.6
6	Diameter of the gas inlet, d_s	12.5
7	Length of the contactor	2030.0

to minimize the effect due to liquid leaving the system or air–liquid separation. There were three outlets provided at the top, bottom and centre of the separator. The bottom and centre outlets allowed liquid to come out while the top outlet allowed air to come out of the separator. By operating the valves V_6 and V_8 (figure 1), the liquid level inside the separator can be maintained. The front and back of the separator are fitted with transparent perspex sheets to enable the inside of the separator to be viewed.

3. EXPERIMENTAL TECHNIQUE

The nozzle, the ejector assembly and the contactor were perfectly aligned in a vertical position to obtain an axially symmetric jet. The nozzle was fixed at the optimum position at a distance of one throat diameter from the entry of the throat. This distance was decided from our earlier experiments (Datta 1976). The experimental procedure is explained on the basis of sketches shown in figure 2(a)–2(e). In all experiments the suction port V_5 of the ejector was always kept open.

(a) To start with, valves V_6 and V_8, shown in figure 1, were kept in a fully open position. When the pump was started and valves V_3 and V_4 were adjusted to the desired liquid flow, the jet, after leaving the nozzle, directly hit the bottom of the air–liquid separator and the liquid cleared out from the bottom valve, V_8 [figure 2(a)]. There was neither any suction from suction port V_8 nor any change in manometer readings, M_1 to M_9. The jet energy remained totally unused.

(b) Valve V_8 was then closed and the liquid flowing in as a jet was allowed to accumulate in the separator up to some height. The above valve was then adjusted to maintain a constant liquid height in the separator, as shown in figure 2(b). It was observed that when the jet plunged into the accumulated column of liquid, there was an intense mixing zone of gas and liquid. The air–liquid mixture moved downwards a certain distance depending on the jet momentum. This was a simple case of a plunging jet system. Also, in this case the manometers attached to the system did not show any change. This phenomenon was observed at other liquid heights until the liquid level reached the point "t" [figure 2(c)], which is the point where the liquid level touches the extended vertical contactor.

(c) When the liquid height reached the point "t", it was seen that there was a sudden change in the suction characteristics of the secondary air due to the arresting of the jet inside the pipe line contactor. At this liquid level there was suction of air from the secondary inlet of the ejector. The two phases moved co-currently through the ejector diffuser, pipeline contactor and mixed after the jet plunged into the liquid. Under this condition, a continuous positive flow of air was obtained in the system. The manometers connected to the system showed positive deflection.

Table 2. Dimensions of the nozzles

Nozzle No.	Nozzle diameter, d_n (mm)	Area ratio, A_r
1	3.96	169.78
2	4.76	117.51
3	5.55	86.44
4	6.35	66.03
5	7.93	42.34
6	9.53	29.32

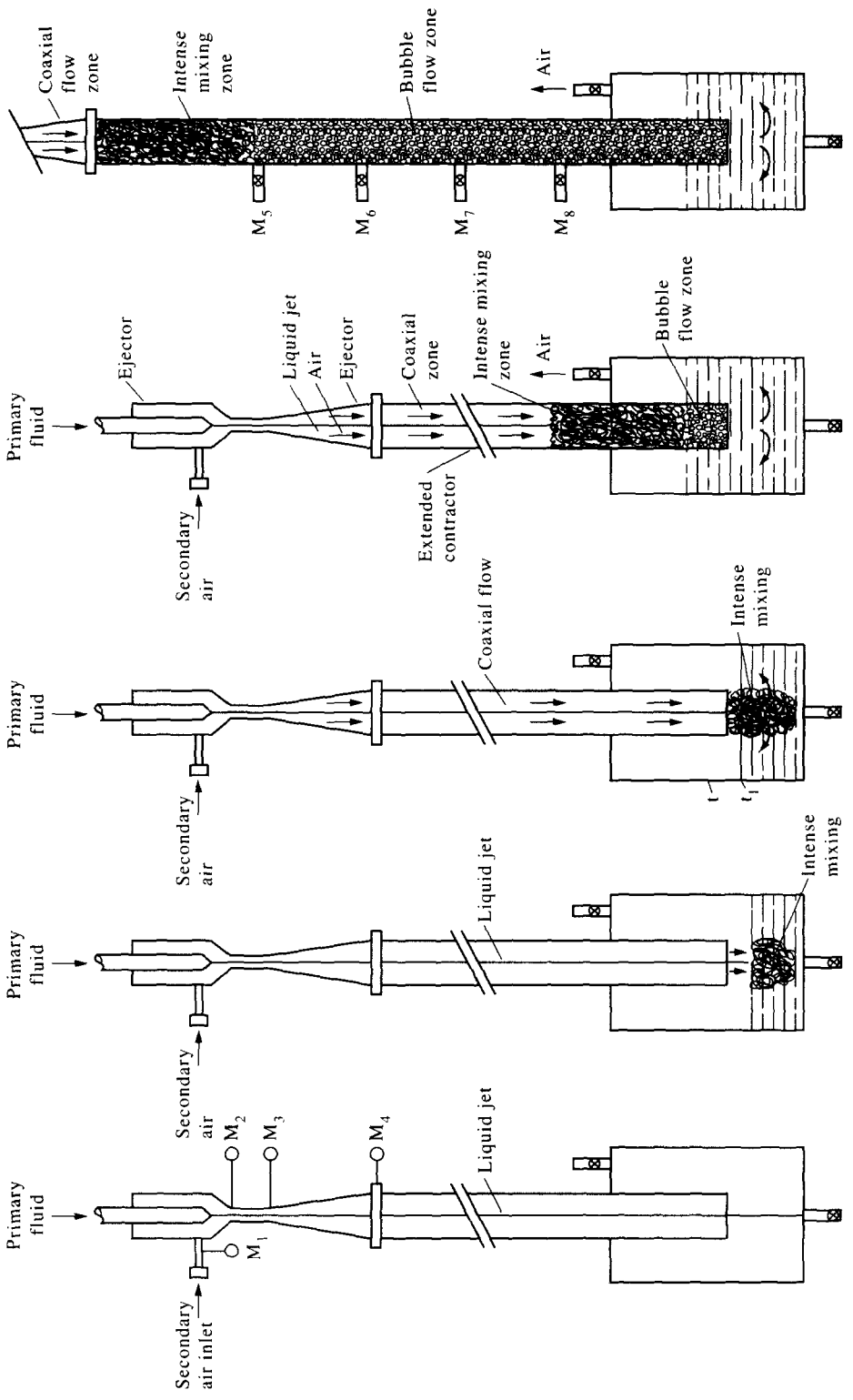

Figure 2. Experimental procedure.

Table 3. Physical properties of the fluids, temperature of measurement −30°C

Sl. No.	Fluid	Density, ρ (kg/m^3)	Viscosity, μ (kg/m s)	Surface tension, σ (N/m)
1	water	995.7	0.797×10^{-3}	0.0710
2	kerosene	829.5	2.991×10^{-3}	0.0292
3	paraffin	808.9	5.682×10^{-3}	0.0290
4	air	1.165	1.863×10^{-3}	—

(d) When the liquid level was further increased [figure 2(d)], by adjusting the valves V_6 and V_8, the jet plunged in the liquid inside the extended contactor. Two distinct zones were observed in the contactor at this stage: an intense gas–liquid mixing zone followed by a downflow fine bubble zone. The intense gas–liquid mixing zone is the zone where the jet penetrates the liquid, releases its energy and disperses the gas. The two-phase downflow bubble zone was due to the entrainment of bubbles from the intense zone by the downflowing liquid. Figure 2(e) shows the column when it is filled with gas–liquid mixture in which the top portion is the intense mixing zone followed by a very uniform bubble zone.

It has been found that increasing the liquid level in the column may lead to flooding of the ejector. This is not desirable because submergence of the nozzle leads to a decrease in the performance of the ejector.

In actual experiment, when a steady flow of gas and liquid was obtained in the column and the two-phase downflow bubble zone became steady, pressure drop between the two points in the zone was noted. For measuring the gas–liquid holdup in the system the solenoid valves SV_1 and SV_3 (figure 1) were switched off simultaneously, which caused an immediate termination of flow. The liquid–gas mixture inside the column arrested and was allowed to settle for some time. The liquid height inside the column was then noted, from which the holdup of gas in the column can be obtained. Experiments were conducted with five different nozzles (table 2) and with air–water,

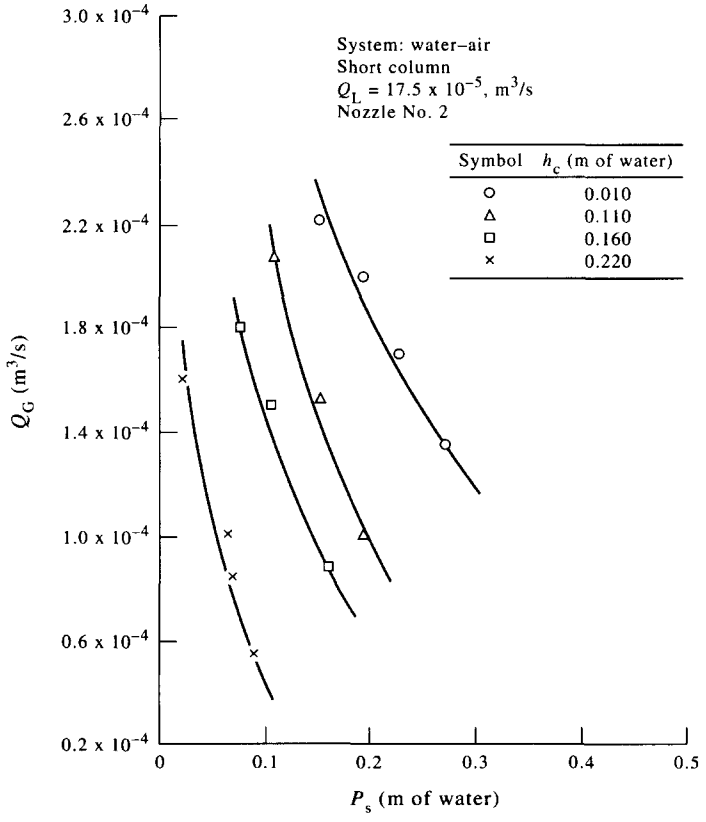

Figure 3. Effect of height of liquid column on air entrainment.

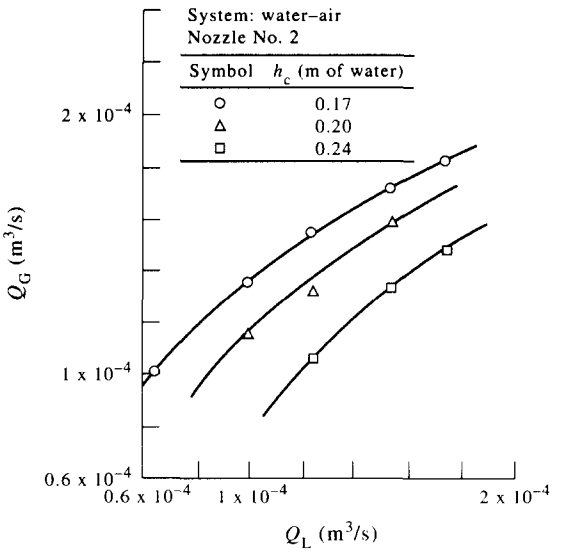

Figure 4. Variation of air entrainment with jet energy.

air–kerosene and air–paraffin (table 3) systems. The ranges of flow rates used for the liquids were as follows:

$$\begin{cases} \text{water flow rate,} & (0.07\text{–}0.34) \times 10^{-3}\ \text{m}^3/\text{s} \\ \text{kerosene flow rate,} & (0.03\text{–}0.22) \times 10^{-3}\ \text{m}^3/\text{s} \\ \text{paraffin flow rate,} & (0.02\text{–}0.24) \times 10^{-3}\ \text{m}^3/\text{s}. \end{cases}$$

The amount of air entrained by the above liquid flow rates varied from 0.16×10^{-6} to $360.0 \times 10^{-6}\ \text{m}^3/\text{s}$. The experiments were carried out in the temperature range of 30 ± 1°C. The physical properties of the liquids were measured by standard techniques.

4. RESULTS AND DISCUSSION

In the present system it is obvious that jet energy is being utilized in air entrainment, gas–liquid mixing, overcoming friction loss in two-phase downflow, developing pressure in the separator for maintaining a particular height of liquid in the column. Some of the typical experimental results are given. Figure 3 shows that for a particular nozzle, water flow rate and liquid height in the column, the entrainment of air decreases with the increase of separator pressure, P_s. Similarly, figure 4 shows that for a particular nozzle and height of liquid in the column, the air entrainment increases with the liquid flow rate, when the separator pressure is constant.

The variation of gas-phase holdup fraction, ϵ_G, with flow ratio, ϕ_R, for different nozzles and different systems shown in figure 5, are typical of all other cases. At a low value of ϕ_R, ϵ_G increases rapidly with increase in ϕ_R. Beyond a certain value of ϕ_R, ϵ_G remains practically constant.

Kulkarni & Shah (1984), with their studies in a downflow bubble column with a sparger type system, showed the zones where operation is not possible. It is interesting to find in the present system that operation is possible in regime "B" (figure 6) and the air flow is much more compared to their system. The zone of operation of Bando *et al.* (1988) has also been compared in this figure and found to be much lower with respect to the present work.

4.1. Analysis of pressure drop

The prediction of two-phase gas–liquid frictional pressure drop in downflow is not possible by theoretical analysis alone because the phenomena of momentum transfer between the phases, the wall friction and the shear at the phase interface cannot be specified quantitatively. Moreover, if the boundary conditions are not defined it is difficult to analyse the two-phase pressure drop theoretically. In practice, use is therefore made of relationships based on models which are

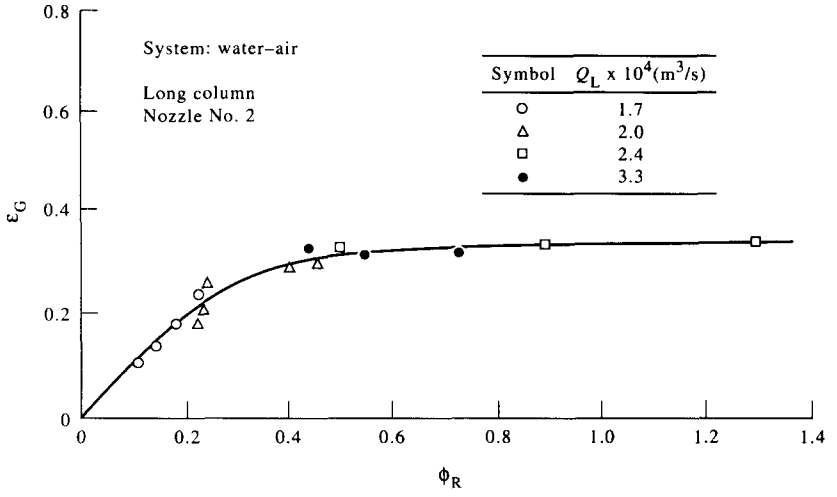

Figure 5. Effect of dispersed phase flow rate on the dispersed phase holdup fraction at different continuous phase flow rates.

corrected or correlated by measurements. In the present case, therefore, the two-phase downflow pressure drop data have been analysed by similarity analysis.

Similarity analysis has been approached by considering the equations of motion of liquid and the boundary conditions in a bubble for stable flow. The analysis has been carried out for the zone where uniform two-phase bubble flow is prevalent. Assuming one-dimensional steady flow, the equation of motion for the liquid in steady state is,

$$V_{Lx}(\delta V_{Lx}/\delta x) = -(1/\rho_L)(\delta p_L/\delta x) + (\mu_L/\rho_L)[(1/r)(\delta/\delta r)(r\delta V_{Lx}/\delta r)] + g \qquad [1]$$

where

V_{Lx} = velocity of liquid at any x (m/s)
x = any height from datum (m)
ρ_L = density of the liquid (kg/m^3)
p_L = pressure of the liquid (N/m^2)
μ_L = viscosity of the liquid (kg/m s)

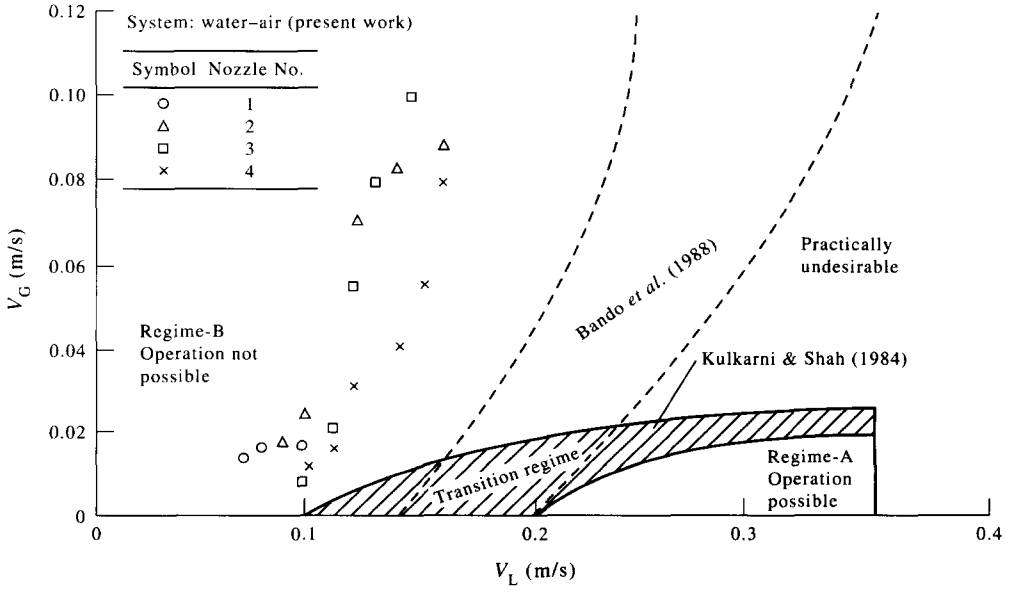

Figure 6. Regime map of stable co-current downflow.

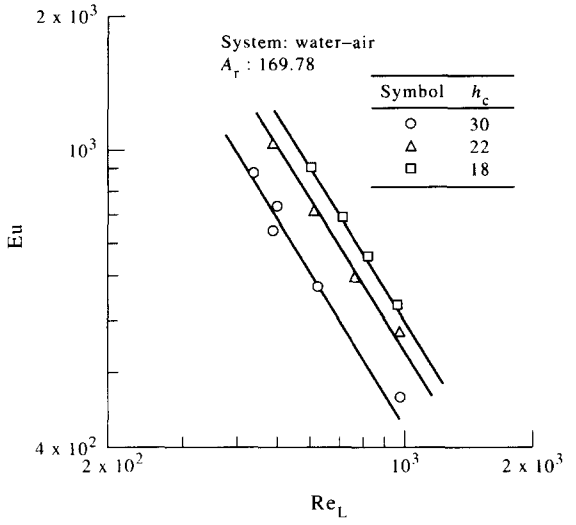

Figure 7. Variation of Euler number with liquid flow rates at different heights of liquid column.

r = radius from the jet axis (m)
g = acceleration due to gravity (m/s^2)

Since the gas phase is dispersed and discontinuous, the equation of motion for gas is not applicable here. However, the boundary condition at the bubble surface is given by

$$p_L + \mu_L(\delta V_{Lx}/\delta x) = p_G + (\sigma_L/r_b) + \mu_G(\delta V_G/\delta r) \quad [2]$$

where

p_G = pressure of the gas (N/m^2)
σ_L = surface tension of the liquid (N/m)
r_b = radius of the bubble (m)
μ_G = viscosity of the gas (kg/m s)
V_G = superficial velocity of the gas (m/s)

which is obtained by balancing the normal stress at the gas–liquid interface.

Introducing the following dimensionless functions,

$$\bar{V}_L = (V_{Lx}/V_L), \quad X = (x/h_c)$$

$$p_L = [p_L/\{(\Delta P_T/\Delta z)d_c\}], \quad R = (r/d_n),$$

$$R_b = (r_b/d_c).$$

where

$\bar{V}_L$ = dimensionless velocity, V_{Lx}/V_L
P_L = dimensionless pressure of the liquid
R_b = dimensionless radius of the bubble
X = dimensionless height, x/h_c
R = dimensionless radius, r/d_c
ΔP_T = pressure drop in the contactor (N/m^2)
Δz = distance between pressure tappings (m)
d_c = diameter of the contactor (m)
h_c = height of the liquid inside the contactor (m)
d_n = diameter of the nozzle (m)

and substituting them into [1] one gets,

$$(V_L^2/h_c)[\bar{V}_L(\delta\bar{V}_L/\delta X)] = -(1/\rho_L)(\Delta P_T d_c/\Delta z h_c)(\delta P_L/\delta X) + (\mu_L/\rho_L)\{(V_L/Rd_n^2)\delta/\delta R(R\delta\bar{V}_L/\delta R)\} + \boldsymbol{g} \quad [3]$$

which may be written as,

$$[0(1)] = -(\Delta P_T d_c/\Delta z \rho_L V_L^2)[0(1)] + (\mu_L/\rho_L V_L d_n)(h_c/d_c)[0(1)] + \boldsymbol{g}h_c/V_L^2 \quad [4]$$

In the above equation the terms in brackets [ ] are of the order of unity. Again substituting the dimensionless function in [2], one gets,

$$(\Delta P_T/\Delta z)d_c[P_L] + (\mu_L V_L/h_c)[\delta V_L/\delta x] = (\Delta P_T/\Delta z)d_c[p_G] + (\sigma_L/d_c)[1/R_b] \quad [5]$$

or,

$$(\Delta P_T d_c/\Delta z \rho_L V_L^2)[0(1)] + (\mu_L V_L/h_c \rho_L V_L^2)[0(1)] = (\Delta P_T d_c/\Delta z \rho_L V_L^2)[0(1)] + (\sigma_L/d_c \rho_L V_L^2)[0(1)] \quad [6]$$

Hence the non-dimensional groups important in the two-phase downflow are:

$$(\Delta P_T d_c/\Delta z \rho_L V_L^2),\ (\mu_L/\rho_L V_L d_n),\ (\mu_L/\rho_L V_L h_c),\ (h_c/d_c),\ (\boldsymbol{g}h_c/V_L^2) \text{ and } (\sigma_L/d_c \rho_L V_L^2).$$

In these groups it may be said that, except for the Euler number, Eu, i.e. $\Delta P_T d_c/\Delta z \rho_L V_L^2$, all are independent groups, hence,

$$\mathrm{Eu} = \lambda_1[(\mu_L/\rho_L V_L d_n)(\mu_L/\rho_L V_L h_c)(h_c/d_c)(\boldsymbol{g}h_c/V_L^2)(\sigma_L/d_c \rho_L V_L^2)] \quad [7]$$

The groups above may be rearranged as follows,

$$\mathrm{Re}_L = (\rho_L V_L d_c/\mu_L) = (\rho_L V_L d_n/\mu_L) \times (d_c/d_n)$$

$$A_r = (d_c/d_n)^2 = 1/[(\mu_L/\rho_L V_L h_c) \times (\rho_L V_L d_n/\mu_L) \times (h_c/d_c)]^2$$

$$H_r = (h_c/d_c)$$

$$\mathrm{Su} = (\sigma_L \rho_L d_c/\mu_L^2) = (\sigma_L/d_c \rho_L V_L^2) \times (\rho_L V_l d_c/\mu_L)^2$$

$$\mathrm{Mo} = (\rho_L \sigma_L^3/\boldsymbol{g}\mu_L^4) = (\sigma_L/d_c \rho_L V_L^2)^3 \times (\rho_L V_L d_c/\mu_L)^4 (h_c/d_c) \times (V_L^2/\boldsymbol{g}h_c)$$

Hence [7] may be rewritten as,

$$\mathrm{Eu} = \lambda_2[\mathrm{Re}_L, A_r, H_r, \mathrm{Su}, \mathrm{Mo}] \quad [8]$$

Here

λ_2 = function of a dimensionless group
Re_L = Reynolds number of the liquid based on the contactor diameter, $\rho_L V_L d_c/\mu_L$
A_r = area ratio of contactor to nozzle $(d_c/d_n)^2$
H_r = height ratio of the liquid column inside the contactor to the diameter of the contactor (h_c/d_c).

The Suratmann number, Su, is a combination of the Reynolds and Weber groups and signifies the balance of three forces, viz. inertia, surface tension and viscous forces, which accounts for the bubble behaviour in different column sizes. The Morton number, Mo, is a combination of the Weber, Reynolds and Froude groups for the continuous phase and signifies a complex balance between the viscous, interfacial tension and gravitational forces which cause the gas bubbles to behave hydrodynamically different from a rigid solid sphere.

4.2. Correlation of Eu

In order to find the functional relation between Eu and other parameters, log–log plots of Eu against

—Re_L for constant A_r and H_r,
—A_r for constant Re_L and H_r,
—H_r for constant A_r and Re_L,

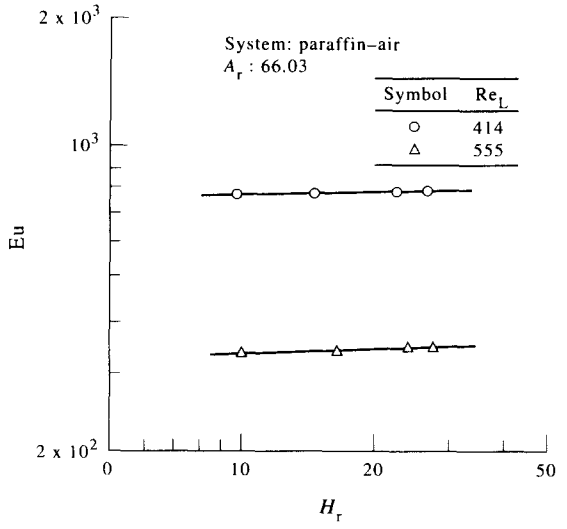

Figure 8. Variation of Euler number with height ratio at different liquid flow rates.

were made in figures 7, 8 and 9, respectively. In the range of experimentation the relations are linear, hence [8] may be written as

$$\mathrm{Eu} = c_1\,\mathrm{Re}_\mathrm{L}^{b_1} A_\mathrm{r}^{b_2} H_\mathrm{r}^{b_3}\,\mathrm{Su}^{b_4}\,\mathrm{Mo}^{b_5} \qquad [9]$$

Equation [9] was fitted to the experimental data by multiple linear regression. Calculations were done using the least squares technique. This leads to

$$\mathrm{Eu} = 0.11 \times 10^8\,\mathrm{Re}_\mathrm{L}^{-2.15} A_\mathrm{r}^{-0.07} H_\mathrm{r}^{0.09}\,\mathrm{Su}^{-1.71}\,\mathrm{Mo}^{-1.33} \qquad [10]$$

A plot of the experimental data and calculated values of Eu from [10] is shown in figure 10.

4.3. Correlation of ϵ_G

The gas-phase holdup fraction, ϵ_G, has also been correlated in a similar fashion,

$$\epsilon_\mathrm{G} = \lambda_3(\mathrm{Re}_\mathrm{L}, A_\mathrm{r}, H_\mathrm{r}, \mathrm{Su}, \mathrm{Mo}) \qquad [11]$$

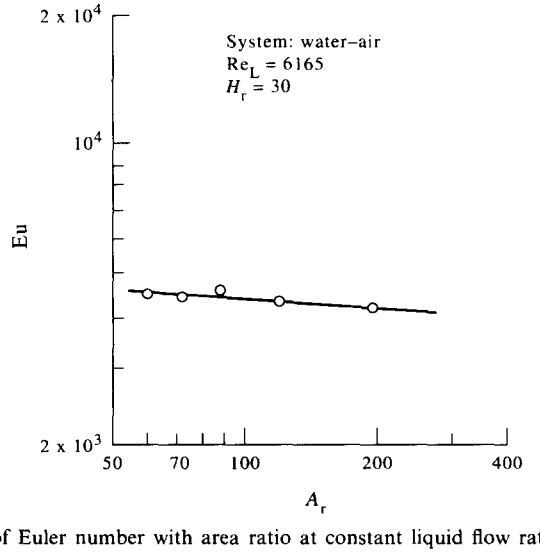

Figure 9. Variation of Euler number with area ratio at constant liquid flow rates and height ratios.

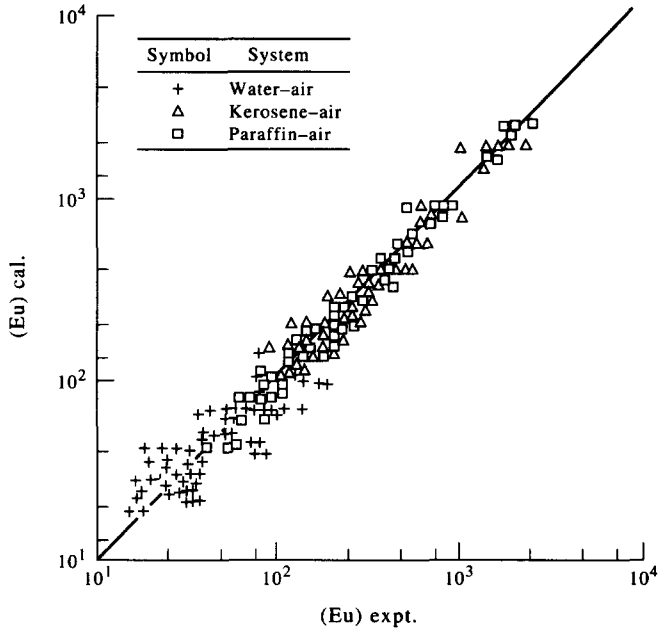

Figure 10. Comparison of the experimental values of Euler number with those calculated from [10].

Now since there is a limiting condition for ϵ_G, i.e.

$$\text{when} \quad Q_G = 0, \quad \epsilon_G = 0 \text{ and}$$

$$\text{when} \quad Q_L = 0, \quad \epsilon_G = 1$$

hence suggesting the following functional form of the holdup correlation:

$$\epsilon_G = 1 - \exp(-c_2 \, Re_L^{b_6} \, A_r^{b_7} H_r^{b_8} \, Su^{b_9} \, Mo^{b_{10}}) \qquad [12]$$

This is because of the linear variation of $-\ln(1-\epsilon_G)$ with respect to Re_L, H_r and A_r (figures 11, 12 and 13) on a log–log scale.

Rearranging and simplifying, [12] becomes,

$$-\ln(1-\epsilon_G) = c_2 \, Re_L^{b_6} \, A_r^{b_7} H_r^{b_8} \, Su^{b_9} \, Mo^{b_{10}} \qquad [13]$$

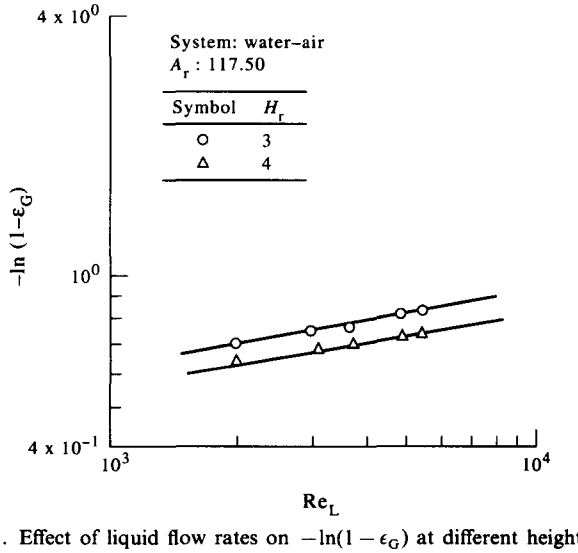

Figure 11. Effect of liquid flow rates on $-\ln(1-\epsilon_G)$ at different height ratios.

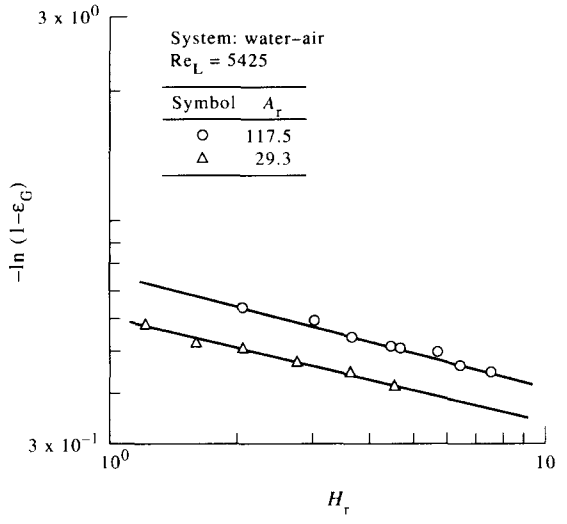

Figure 12. Effect of height ratio on $-\ln(1-\epsilon_G)$ at different area ratios.

Equation [13] was fitted to the 1270 sets of data by multiple linear regression. The calculation was performed using the least squares technique. This gives,

$$\epsilon_G = 1 - \exp(-6.87 \times 10^{-3}\, \mathrm{Re}_L^{0.16}\, A_r^{0.17} H_r^{-0.22}\, \mathrm{Su}^{1.15}\, \mathrm{Mo}^{0.58}) \qquad [14]$$

A plot of the experimental and the calculated values of ϵ_G is shown in figure 14 for all systems. The range of variation of the different parameters for both the Eu and ϵ_G correlations is as follows:

$$88 < \mathrm{Re}_L < 10481$$

$$29.03 < A_r < 169.78$$

$$1 < H_r < 31$$

$$0.375 \times 10^5 < \mathrm{Su} < 0.574 \times 10^7$$

$$0.111 \times 10^{-10} < \mathrm{Mo} < 0.517 \times 10^{-6}.$$

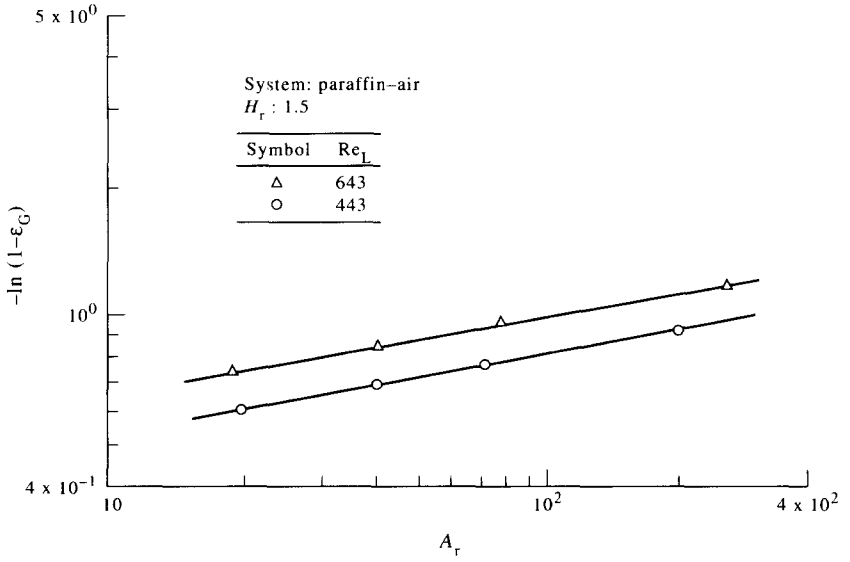

Figure 13. Effect of area ratio on $-\ln(1-\epsilon_G)$ at different liquid flow rates.

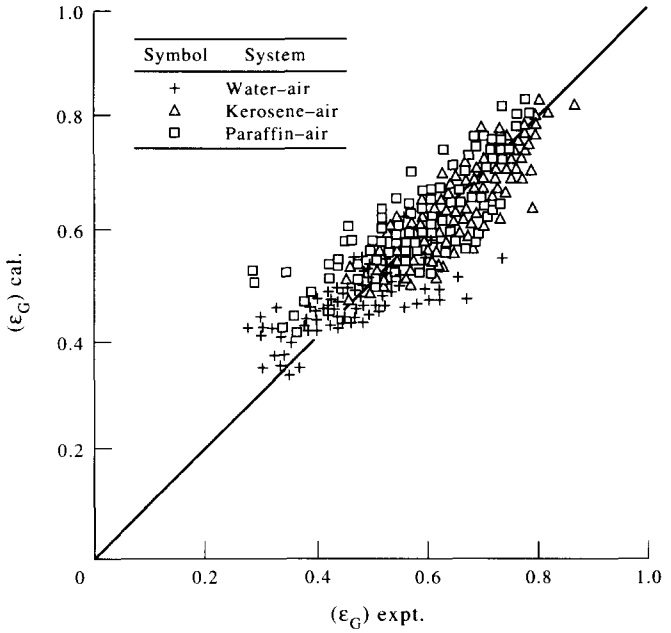

Figure 14. Comparison of the experimental values of the gas-phase holdup fraction with those calculated from [14].

5. CONCLUSION

In this paper an attempt has been made to correlate the two-phase pressure drop per unit length of contactor and the dispersed phase holdup fraction in a gas–liquid co-current downflow bubble column fitted with an ejector as a function of various dimensionless groups obtained through similarity analysis. Correlations have been found to be satisfactory within the range of the experiments.

REFERENCES

Bando, Y., Kuraishi, M., Nishimura, M., Hattori, M. & Asada, T. 1988 Cocurrent downflow bubble column with simultaneous gas–liquid injection nozzle. *J. Chem. Engng Japan* **21,** 607–612.

Ben Brahim, A., Prevost, M. & Bugarel, R. 1984 Momentum transfer in a vertical down flow liquid jet ejector: case of self gas aspiration and emulsion flow. *Int. J. Multiphase Flow* **10,** 79–94.

Burgess, J. M., Molloy, N. A. & McCarthy, M. J. 1972 A note on the plunging liquid jet ejector. *Chem. Engng Sci.* **27,** 442–445.

Burgess, J. M. & Molloy, N. A. 1973 Gas absorption in the plunging liquid jet ejector. *Chem. Engng Sci.* **28,** 183–190.

Datta, A. K. 1976 Effect of mixing throat length on the performance of a liquid jet ejector. M.Sc. thesis, Chemical Engineering Department, IIT, Kharagpur, India.

Herbrechtsmeier, P., Schäfer, H. & Steiner, R. 1981 Gas absorption in downflow bubble columns for the ozone–water system. *Ger. Chem. Engng* **4,** 258–264.

Kulkarni, A. & Shah, Y. T. 1984 Gas phase dispersion in a downflow bubble column. *Chem. Engng Commun.* **28,** 311–326.

Mukherjee, D., Biswas, M. N. & Mitra, A. K. 1988 Hydrodynamics of liquid–liquid dispersion in ejectors and vertical two phase flow. *Can. J. Chem. Engng* **66,** 896–907.

Ohkawa, A., Shiokawa, Y., Sakai, N. & Endoh, K. 1985 Gas holdup in downflow bubble columns with gas entrainment by a liquid jet. *J. Chem. Engng Japan* **18,** 172–174.

Rao, V. G., Raju, R. S., Amarnath, M. S. & Varma, Y. B. G. 1983 Hydrodynamics of two phase co-current down flow through packed bed. *AIChE Jl* **29,** 467–473.

Schügerl, K. 1985 Nonmechanically agitated bioreactor systems. In *Comprehensive Biotechnology* (Edited by Moo-Young), Vol. 2, Section 1, Chap. 5. Pergamon Press, New York.

Van de Donk, J. A. C., Van der Lans, R. G. J. M. & Smith, J. M. 1979 The effect of contaminants with oxygen transfer rate achieved with a plunging jet reactor. *Third European Conf. on Mixing (BHRA)*, York, England, F1, pp. 289–302.

Van de Sande, E. & Smith, J. M. 1976 Jet break up and air entrainment by low velocity turbulent water jets. *Chem. Engng Sci.* **31,** 219–224.

Velan, M. & Ramanujam, T. K. 1991 Hydrodynamics of a reverse flow jet loop bioreactor. *Ind. Chem. Engng* **33,** 80–84.